Published in final edited form as:
Nature. 2008 July 17; 454(7202): 291–296. doi:10.1038/nature07118.

Positive feedback of G1 cyclins ensures coherent cell cycle entry

Jan M. Skotheim[*], **Stefano Di Talia**[*], **Eric D. Siggia**[*], and **Frederick R. Cross**[+]

[*] Center for Studies in Physics and Biology, The Rockefeller University, 1230 York Ave., New York, NY 10021, USA

[+] The Rockefeller University, 1230 York Ave., New York, NY 10021, USA

Abstract

In budding yeast, the Start checkpoint integrates multiple internal and external signals into an all-or-none decision to enter the cell cycle. Here, we show that Start behaves like a switch due to systems-level feedback in the regulatory network. In contrast to current models proposing a linear cascade of Start activation, transcriptional positive feedback of the G1 cyclins Cln1,2 induces the near-simultaneous expression of the ~200-gene G1/S regulon. Nuclear Cln2 drives coherent regulon expression, while cytoplasmic Cln2 drives efficient budding. *cln1,2*-deleted cells frequently arrest as unbudded cells, incurring a large fluctuation-induced fitness penalty due to both the lack of cytoplasmic Cln2 and insufficient G1/S regulon expression. Thus, positive-feedback-amplified expression of Cln1,2 simultaneously drives robust budding and rapid, coherent regulon expression. A similar G1/S regulatory network in mammalian cells, comprised of non-orthologous genes, suggests either the conservation of regulatory architecture or convergent evolution.

Positive feedback in genetic control networks can ensure that cells do not slip back and forth between either cell cycle phases or developmental fates. For example, commitment to sporulation in budding yeast is driven by transcriptional positive feedback of the meiotic inducer *IME1*[1–3]. In *Xenopus laevis*, positive feedback underlies the all-or-none characteristics of oocyte maturation[4, 5] and mitotic entry[6, 7], suggesting the frequent use of positive feedback to regulate cellular transitions.

Absent from this list of examples is the well-studied Start checkpoint controlling cell cycle commitment in budding yeast. Nutrient limitation and pheromone exposure arrests cells prior to DNA replication, while size control extends G1 in small daughter cells[8–11]. Beyond Start, cells proceed through division almost independently of size and environment[9]. Previous experiments suggested that Start represents a feedback-free cascade of events[12] (see schematic in Fig. 1a; omitting red arrows). The transition is initiated by the G1-cyclin Cln3[13–15], which in complex with Cdc28 activates the transcription of about 200 genes[16] by phosphorylating promoter-bound protein complexes that include the transcription factors SBF and MBF[17] and the transcriptional inhibitor Whi5[18, 19]. Phosphorylation and inactivation of Whi5 is rate-limiting, and phosphorylated Whi5 rapidly exits the nucleus. The G1/S regulon, which includes two additional G1-cyclins, *CLN1,2*, contributes to the activation of B-type cyclins, DNA replication, spindle pole body duplication, and bud emergence. Mitotic B-type cyclins then inactivate SBF[20] and, with *NRM1*, inactivate MBF[21], thus turning off the G1/S regulon.

Correspondence and requests for materials should be addressed to J.M.S. (e-mail: jskotheim@rockefeller.edu).

Any one of the three G1-cyclins suffices to activate the regulon, suggesting the potential for transcriptional positive feedback of *CLN1,2* on their own expression[22, 23]. However, analysis of synchronized populations led to the conclusion that positive feedback, defined as Cln1,2 advancing transcription from the *CLN2* promoter, did not occur in WT; rather, Cln3 was the sole activator of firing[14, 15].

In sharp contrast to the prevailing linear model, we demonstrate that Cln1,2-dependent positive feedback is central to Start control. We use single-cell time-lapse fluorescent microscopy to show that Cln1,2 advance timing and reduce variability in the activation of *CLN2*, and of the entire G1/S regulon. We further explore the mechanisms and functional significance of this control.

Positive Feedback of G1-Cyclins

Positive feedback of Cln1,2 on their own transcription should yield faster accumulation of *CLN2* mRNA in WT cells than in *cln1*Δ *cln2*Δ cells. Although Cln1,2-dependent positive feedback was clearly demonstrated in the absence of Cln3[22–24], this does not imply that WT cells function similarly. In synchronized populations, near-identical timing of onset of *CLN2* promoter activity was observed in the presence or absence of *CLN1,2*, leading to the linear model[14, 15]. Here, we revisit this issue using single cell assays. As a reporter for *CLN2* transcription, we use unstable GFP driven by the *CLN2* promoter24, [25] (see Methods and Fig S1–2). Birth time was determined using a marker for cytokinesis (disappearance of the Myo1-GFP myosin ring[11], which did not influence the *CLN2pr-GFP* signal). The timing of *CLN2* promoter induction in individual cells is sharp and easily quantified computationally (see Methods, Fig 1d,e and Fig. S1–2). Since *cln1*Δ *cln2*Δ cells are larger than WT, we integrated *MET3pr-CLN2* in both strains, to conditionally express Cln2 prior to time-lapse imaging so that initially sizes were comparable[14] (see methods; Fig. S3&S12 for controls). Thus, we can assay for positive feedback by comparing the time interval from birth to transcriptional activation of *CLN2pr-GFP* transcription in the first cell cycle after *MET3pr-CLN2* turnoff in WT and *cln1*Δ *cln2*Δ cells.

Positive feedback should advance *CLN2* promoter activation in WT compared to *cln1*Δ *cln2*Δ cells[14, 15]. Strikingly, in daughter cells, the average time between birth and *CLN2* promoter activation (τ_{on}; Fig. 1d–e,f) was much shorter for WT (41 min) than for *cln1*Δ *cln2*Δ (83 min). Furthermore, *CLN2pr-GFP* activation was much less variable for WT than for *cln1*Δ *cln2*Δ cells (standard deviation of 21 vs. 47 min). *CLN2pr-GFP* transcription was Cln3-dependent in *cln1*Δ *cln2*Δ cells. Qualitatively similar results were obtained in mother cells and also in cells growing in glycerol/ethanol instead of glucose. In all cases, the interval from birth to *CLN2pr-GFP* activation was smaller and less variable in WT than in *cln1*Δ *cln2*Δ, indicating strong positive feedback of Cln1,2 on their own transcription independent of nutrient conditions or cell type (Table S3; $P < 10^{-4}$).

We explored the potential redundancy of *CLN1* and *CLN2* in activating the feedback loop. Although budding is slightly delayed in *cln1*Δ *CLN2*, and *CLN1 cln2*Δ cells compared to WT, the timing of *CLN2* promoter activation is similar (Table S3), indicating that *CLN1* and *CLN2* form redundant conduits for positive feedback.

Our data can be reconciled with previous work[14, 15] arguing against positive feedback because measurements averaged over a population of cells necessarily lose information. In addition to delayed onset of transcription, *cln1*Δ *cln2*Δ cells express a more intense and prolonged *CLN2pr-GFP* signal. The larger peaks are likely due to a delay in the Clb2-mediated repression of SBF/MBF[14, 15, 20, 21] (Fig. 1d–e), since the average time between induction of *CLN2* and *CLB2* was much larger in *cln1*Δ*cln2*Δ strains, (measured using a

CLB2pr-GFP cassette) (Fig. 1f; Fig. S13), and Clb2p accumulation is known to be delayed in *cln1*Δ*cln2*Δ strains[14].

Therefore, imperfect synchrony[11] allows the high and lengthened transcriptional response from the first *cln1*Δ*cln2*Δ cells firing the *CLN2* promoter to mask the delayed response of the majority. This effect is reconstituted in Fig. 1g by averaging our measured single-cell data, and explains why positive feedback was not detected in measurements of mRNA levels in populations of synchronized daughter cells[14, 15].

Coherent Regulon Expression

Once a cell senses the signal to initiate the cell cycle, it must actuate all the machinery effecting the cell cycle transition. At Start, this requires activating many SBF and MBF regulated genes[16] encoding proteins involved in DNA replication and bud site formation. However, noise in protein expression in individual cells[26] could interfere with expression of this large regulon. In particular, the delayed and variable induction of the *CLN2* promoter in *cln1*Δ *cln2*Δ cells suggested that G1/S regulon expression might be severely disrupted in these feedback-free cells.

To investigate regulon expression in individual cells, we compared induction of *CLN2pr-GFP* and *RAD27-mCherry*, another member of the regulon[16] (Fig. 2a–d; Fig. S7–8). *RAD27* expression is Cln-dependent (Fig. S11). *CLN2* and *RAD27* are synchronously induced in WT, while there is a long and variable period of time between the inductions of the two genes in the *cln1*Δ *cln2*Δ mutant (Fig. 2e–f). Indeed, out of the 86 *cln1*Δ *cln2*Δ cells studied, 11 failed to produce a detectable increase in Rad27-mCherry and 4 failed to produce a detectable increase of either marker. We performed identical experiments on strains containing *CLN2pr-GFP* and *RFA1-mCherry*, another regulon member[16], and obtained similar results (Fig. 2g–h). Our conclusions are valid even after excluding outlying points ($P<0.01$). Thus, Cln1/2 dependent positive feedback likely promotes coherent and efficient transcription across the SBF/MBF regulon.

Further comparison of these three promoters in *cln1*Δ *cln2*Δ cells reveals that *CLN2* is almost always the first of the three to be activated, while the times to subsequent *RFA1pr* and *RAD27pr* inductions are significantly different from each other ($P=0.004$; Table S3). This suggests that the *CLN2* promoter is the easiest for Cln3 to induce, followed by the *RFA1* promoter, followed by the *RAD27* promoter. We note that two MBF targets[27–29], *RAD27* and *RFA1*, exhibit different induction timing.

To ask whether lack of coherence in *cln1*Δ *cln2*Δ cells might simply come from low G1 cyclin levels, we analyzed *cln1*Δ *cln2*Δ *6xCLN3* cells. Although expression of both the *CLN2* and *RAD27* promoters was significantly accelerated by extra *CLN3*, these cells still exhibited strongly incoherent expression compared to WT (Fig 2i).

To directly short-circuit the proposed positive feedback loop, we examined gene expression in *cln1*Δ *cln2*Δ *cln3*Δ *MET3pr-CLN2* cells on methionine-free medium (*MET3pr-CLN2* on). Although induction of *CLN2pr-GFP* and *RAD27-mCherry* were strongly accelerated by constitutive *CLN2* expression, incoherent expression compared to WT was still observed (Fig. 2j). Intriguingly, this incoherence was due to *RAD27-mCherry* induction prior to *CLN2pr-GFP*, compared to nearly simultaneous expression in WT (-8 ± 2 min compared to 2 ± 1 min; $P<10^{-3}$), perhaps due to differential loading of SBF (*CLN2*) and MBF (*RAD27*) regulated genes[21, 27–30].

Overall, these experiments suggest that the positive feedback architecture is a particularly effective way to promote coherent regulon expression.

Stochastic cell cycle arrest

In addition to exhibiting incoherent gene expression, 26% of *cln1*Δ *cln2*Δ cells fail to bud (Fig. 3a). We hypothesized that incoherent gene expression plays a role in this sporadic unbudded arrest. 20 out of 143 assayed *cln1*Δ *cln2*Δ cells were 'strongly incoherent': they failed to transcribe one or both of their two transcriptional markers (Fig. 2f,h). 90% of the 'strongly incoherent' cells arrested unbudded compared to 26% of all *cln1*Δ *cln2*Δ cells ($P<0.003$; Fig. 3a). Thus, a lack of coherence in the SBF/MBF regulon is a strong predictor of unbudded arrest within the *cln1*Δ *cln2*Δ population. *6X CLN3* reduced unbudded arrest in *cln1*Δ *cln2*Δ cells, perhaps because of accelerated regulon expression (Fig. 2i). Thus, unbudded arrest in *cln1*Δ *cln2*Δ cells may result from highly delayed expression of some regulon members.

We hypothesized that in strongly incoherent cells, activation of only some regulon members might lead to activation of mitotic Clbs, which would then inactivate further SBF/MBF regulated expression[20] (Fig. 1a; Fig. S9). If genes required for budding in the absence of *CLN1,2*, such as *PCL1,2*[31], had not yet been expressed, unbudded arrest might ensue. Indeed, 20/20 arrested *cln1*Δ *cln2*Δ cells contained large amounts of nuclear Clb2-YFP (Fig. 3b–c).

To further test the role of transcription in unbudded arrest, we deleted the rate-limiting SBF inhibitor *CLB2* in a *MET3pr-CLN2 cln1*Δ *cln2*Δ strain and observed a decrease in unbudded arrest from 26% to 13% (Fig. 3d). Additionally, we integrated unphosphorylatable Cdh1 under *GAL* control (*GALL-HA3-CDH1-m11*) into a *cln1*Δ *cln2*Δ *MET3pr-CLN2* strain to induce rapid degradation of all mitotic cyclins upon galactose induction[32]. This reduced the unbudded arrested fraction to 4% in the first cell cycle following GAL induction (Fig. 3d). Since the timing of *CLB2pr-GFP* induction in *cln1*Δ*cln2*Δ cells was similar whether they arrested or not ($P = 0.91$), the unbudded arrest was not due to unusually early *CLB2* induction.

Thus, mitotic cyclins promote unbudded arrest specifically in highly incoherent *cln1*Δ *cln2*Δ cells, probably due to insufficient regulon expression before Clb-dependent SBF/MBF inactivation.

Cln1,2 inactivate the transcriptional inhibitor *WHI5*

We wanted to determine if Cln1,2-dependent positive feedback operated through Whi5, a transcriptional inhibitor of the G1/S regulon[18, 19]. Whi5 inactivation is rate-limiting for *CLN2* transcription and occurs via Cln-dependent phosphorylation, which leads to nuclear exclusion[19].

First, we developed a quantitative assay for nuclear levels of Whi5-GFP by marking the nucleus with *HTB2-mCherry* (histone H2B) and measuring the difference between nuclear and cytoplasmic GFP fluorescence intensity(Fig. 4a–c). Whi5 entered the nucleus rapidly in both WT and *cln1*Δ *cln2*Δ cells. In WT cells, Whi5 also exited very rapidly. In *cln1*Δ *cln2*Δ cells, Whi5 exited much more slowly (Fig. 4d–g,i) consistent with biochemical data showing that Whi5 remains on the *CLN2* promoter longer in *cln1*Δ *cln2*Δ than in WT cells[18]. Since in *cln1*Δ *cln2*Δ *cln3*Δ cells, Whi5-GFP remained nuclear (Fig. 4h), the slow Whi5 exit in *cln1*Δ *cln2*Δ cells is Cln3-dependent (this also excludes photobleaching artefacts). Thus, Cln3 initiates the slow exit of Whi5 from the nucleus, while Cln1/2 rapidly removes the remainder.

Since Whi5 exit and *CLN2* induction are tightly correlated in WT (Fig. 4j), translocation occurs shortly after Whi5 inactivation and coincides with activation of transcriptional

positive feedback. *CLN2* promoter activation and Whi5 exit were less tightly correlated in *cln1*Δ *cln2*Δ cells consistent with the gradual exit of Whi5 (Fig. 4k; Fig. S5–6).

To examine the role of Whi5 phosphorylation in positive feedback and regulon coherence, we used a *WHI5(6A)* allele19 lacking 6 of 12 Cln-dependent phosphorylation sites. Although Whi5(6A) was reported to be constitutively nuclear[19], we observed significant, but slower and incomplete, shuttling of Whi5(6A)-GFP out of the nucleus at Start and again at nuclear division (10/10 cells; Fig. 4l). *CLN2* and *RAD27* induction are less coherent in *WHI5(6A)* than in WT (Fig. 4m; but more coherent than *cln1*Δ *cln2*Δ), correlating with the poor nuclear transport of Whi5(6A). Thus, interfering with the positive feedback loop by reducing the ability of Cln proteins to phosphorylate Whi5 reduces regulon coherence, even with all three G1 cyclins present.

The addition of *WHI5(6A)* to *cln1*Δ *cln2*Δ cells increased the frequency of unbudded arrest from 26% to 51%, consistent with the idea that unbudded arrest is a consequence of incoherent regulon expression in *cln1*Δ *cln2*Δ cells.

Overall, these results strongly suggest that Whi5 is a Cln1,2 substrate in WT cells, and that this phosphorylation contributes to positive feedback. To see if Whi5 was the only such substrate, we compared timing of *CLN2* promoter activation for *whi5*Δ and *cln1*Δ *cln2*Δ *whi5*Δ cells (Fig. S14; Table S3). Deletion of *WHI5* advances *CLN2* promoter induction in both WT and *cln1*Δ *cln2*Δ cells. Since *cln1*Δ *cln2*Δ *whi5*Δ cells delayed *CLN2pr* induction relative to *whi5*Δ cells, Cln1,2 likely act through a Whi5-dependent and a Whi5-independent mechanism to promote positive feedback. Previous results suggested a Whi5-independent Cln3 requirement for SBF activation[19], possibly acting through Swi6[19, 33]; a similar mechanism may be employed by Cln1,2.

Separable Cln2 functions

Cln1,2 are pleiotropic effectors of Start with important nuclear and cytoplasmic functions[34, 35], complicating interpretation of *cln1*Δ *cln2*Δ phenotypes. Therefore, we tested forced-localization *CLN2* alleles, expressed from the wild-type *CLN2* promoter, that restrict Cln2 to either the nucleus (*CLN2-NLS*) or the cytoplasm (*CLN2-NES*)[34]. *cln1*Δ *cln2*Δ *CLN2-NLS* cells exhibit coherent regulon expression (P=0.45 compared to WT), but *cln1*Δ *cln2*Δ *CLN2-NES* cells are highly incoherent compared to WT ($P<10^{-7}$), implying that coherent gene expression is primarily a nuclear function of *CLN2* (Fig. 6a–b; compare to Fig. 2; Table S3).

Consistent with a role of cytoplasmic Cln2 in budding[34, 35], integration of *CLN2-NES* into *cln1*Δ *cln2*Δ cells strongly reduces arrest (to 3%) in spite of less coherent gene expression. Furthermore, exogenous expression of *CLN2* drives cell cycle progression in previously blocked *cln1*Δ *cln2*Δ cells (Fig. S10) and restores viability of *mbp1*Δ *swi4*Δ cells, which lack SBF and MBF and have very low regulon expression[36, 37]. The localization mutants also have different efficacy for relieving unbudded arrest. Integration of *CLN2-NLS* into *cln1*Δ *cln2*Δ cells, providing coherent gene expression, leads to a partial but significant reduction of unbudded arrest (from 26% to 19%; P=0.04).

Thus, cell morphogenesis and budding can be driven by two partially redundant pathways: via cytoplasmic Cln1,234, 38 or other genes in the G1/S regulon such as Pcl1,2[31] (Fig. 6c). Having Cln1,2 coherently activate the G1/S regulon *and* directly drive bud emergence provides a compact solution to ensure efficient and timely morphogenesis and G1/S regulon expression, before subsequent Clb activation.

Discussion

The regulatory architecture of the G1/S regulon provides an effective design to promote coordinated activation. The promoters are pre-loaded during G1 with a complex of factors that are subsequently rapidly activated by phosphorylation[17, 24, 30] removing a potentially rate-limiting step. Furthermore, the upstream cyclin Cln3 is intrinsically more capable of triggering the *CLN2* promoter compared to two other randomly selected promoters from the regulon (*RFA1* or *RAD27*; Fig 2e–h). High sensitivity of *CLN1/2* to Cln3 means that positive feedback from the initial burst of Cln1,2 will ensure that all other genes fire together. Indeed, in our experiments in WT cells, the genes are expressed too synchronously to evaluate which comes first. We find it likely that positive feedback will be a recurring motif within genetic control networks responsible for the coherent temporal coordination of multiple downstream events.

The sharpness of the Start switch, defined by the rapid exclusion of the transcriptional inhibitor Whi5 and the coherent expression of the G1/S regulon, is principally due to *CLN1,2*-dependent positive feedback (Fig. 6c, red lines) rather than a linear Cln3-Whi5-SBF pathway[14, 15, 18, 19]. Our data are inconsistent with the sharpness of Start being primarily due to non-linear increases in *CLN3* translation[39] or nuclear translocation[40], or cooperative phosphorylation of Whi5 by Cln3[19], since these mechanisms all predict a sharp switch in feedback-free *cln1*Δ *cln2*Δ cells.

In budding yeast, Start is a fundamental point of commitment where physiological inputs such as nutrients, mating factor, size and cell type are integrated to produce an all-or-none decision. We show here that positive feedback provides robust switch-like cell cycle entry. Our single-cell data suggest that the point of commitment to the cell cycle, Start, is a very brief interval coinciding with the initiation of positive feedback and Whi5 exclusion. Subsequent Cln-dependent events, such as Sic1 phosphorylation and degradation[41] leading to DNA replication, could then be viewed as dependent on, rather than part of, Start.

This work also provides a molecular basis for understanding the modular structure of G1[11]. Two temporally uncorrelated processes in G1 are separated by the molecular event of Whi5 inactivation and nuclear exit. The upstream module is responsible for cell size control, while the downstream size-independent module actuates cell cycle progression[11]. Here, we showed that rapid Whi5-exit coincides with initiation of Cln1,2-dependent positive feedback. Once feedback is initiated, the rapidly accumulating Cln1,2 likely dominates cellular Cln-kinase activity and Cln3, the rate-limiting upstream activator, is rendered unimportant. In general, we expect modularity, best revealed by single-cell analysis, to be a signature of feedback-driven cellular control networks.

Our systems-level analysis of Start provides a template for further studies of other checkpoints in yeasts or the G1/S transition in mammals. The utility of feedback at Start leads us to expect similar regulatory architecture across eukaryotes, even if the enabling genes are not homologous.

Methods Summary

Strain and plasmid constructions

Standard methods were used throughout. All strains are W303-congenic.

Time-lapse microscopy

Preparation of cells for time-lapse microscopy was performed as previously described[24]. Since mutant cells are larger than WT, we integrated *MET3pr-CLN2* to conditionally

express Cln2[14]. On media lacking methionine (*MET3pr-CLN2* on), cells bud and divide at comparable sizes (Fig. S3). By pre-growing cells without methionine before plating on media containing methionine (*MET3pr-CLN2* off), we are able to begin our time-lapse imaging experiments with similarly sized WT and *cln1*Δ *cln2*Δ cells. We imaged the first Start in cells that were budded at the time of transfer,and that divided least 30 minutes after methionine addition, to allow degradation of Cln2[13, 42] made before *MET3* promoter turnoff.

Image Analysis

Automated image segmentation and fluorescence quantification of yeast grown under time-lapse conditions were performed as previously described11, 24. We added a function to previously described custom software[24] to identify nuclei labeled with Htb2-mCherry (histone). The red signal was smoothed, disconnected fragments were eliminated and the cells with nuclei too small, or dim, or oddly shaped (area vs. minimally enclosed rectangle) were eliminated. After background subtraction, the nucleus was defined to be where the fluorescence was greater than 70% of maximum, which controls for cell variability and vertical movement of the nucleus. The nuclear Whi5-GFP signal was the difference between the average nuclear and cytosolic intensities.

Data Analysis

Fluorescence time series were extracted from movies as previously described[24]. Time-series were fit using smoothing splines (MATLAB) with a smoothing parameter of 0.001. We defined the onset of transcription for a G1/S fluorescent reporter by the maximum in the second derivative that fell between birth and budding (scored separately), which accurately locates rate-changes in spite of noisy data and slow changes in the background fluorescence (Fig. S3–4).

Methods

Strain and plasmid constructions

Standard methods were used throughout. All strains are W303-congenic. In synchronized WT cells, GFP mRNA from the *CLN2* promoter and *CLN2* mRNA follow similar kinetics, and accumulation of cellular fluorescence follows with a slight delay[24]. *WHI5(6A)* and *WHI5(6A)-GFP* strains with modified *WHI5* at the endogenous locus were a gift from M. Tyers. Plasmids for introduction of *CLN2-NES* and *CLN2-NLS* under control of the *CLN2* promoter were obtained from B. Futcher, and integrated at the *ura3* locus in a *cln1*Δ *cln2*Δ background. Histone H2B (*HTB2*) was C-terminally tagged with *mCherry* using PCR-mediated tagging, with the template plasmid pKT355[43] by J. Bean and B. Timney. *RAD27* and *RFA1* were tagged similarly. All other alleles were from laboratory stocks described previously.

Time-lapse microscopy

Preparation of cells for time-lapse microscopy was performed as previously described[24]. Since mutant cells are larger than WT, we integrated *MET3pr-CLN2* to conditionally express Cln2[14]. On media lacking methionine (*MET3pr-CLN2* on), cells bud and divide at comparable sizes (Fig. S3). By pre-growing cells without methionine before plating on media containing methionine (*MET3pr-CLN2* off), we are able to begin our time-lapse imaging experiments with similarly sized WT and *cln1*Δ *cln2*Δ cells. We imaged the first Start in cells that were budded at the time of transfer, and that divided least 30 minutes after methionine addition, to allow degradation of Cln2[13, 42] made before *MET3* promoter turnoff. Briefly, growth of microcolonies was observed with fluorescence time-lapse

microscopy at 30ºC using a Leica DMIRE2 inverted microscope with a Ludl motorized XY stage. Images were acquired every 3 minutes for cells grown in glucose and every 6 minutes for cells grown in glycerol/ethanol with a Hamamatsu Orca-ER camera. Custom Visual Basic software integrated with ImagePro Plus was used to automate image acquisition and microscope control.

Image Analysis

Automated image segmentation and fluorescence quantification of yeast grown under time-lapse conditions were performed as previously described24. Budding was scored visually, and cell birth was scored by the disappearance of Myo1-GFP at the bud neck, generally with single frame accuracy. Background was measured as the average fluorescence of unlabelled cells and subtracted from the measured pixel intensities. We added a function to previously described custom software[24] to identify nuclei labeled with Htb2-mCherry (histone). The red signal was smoothed, disconnected fragments were eliminated and the cells with nuclei too small, or dim, or oddly shaped (area vs. minimally enclosed rectangle) were eliminated. After background subtraction, the nucleus was defined to be where the fluorescence was greater than 70% of maximum, which controls for cell variability and vertical movement of the nucleus. The nuclear Whi5-GFP signal was the difference between the average nuclear and cytosolic intensities.

Data Analysis

P-values using appropriate tests yielded $P<0.001$ for all comparisons in the text, except where noted. Fluorescence time series were extracted from movies as previously described[24]. Time-series were fit using smoothing splines (MATLAB) with a smoothing parameter of 0.001. We defined the onset of transcription for a G1/S fluorescent reporter by the maximum in the second derivative that fell between birth and budding (scored separately). This method was chosen because it accurately locates rate-changes in spite of noisy data and slow changes in the background fluorescence. The onset time was nearly unchanged over a range of 10^3 in smoothing parameter (Fig. S3–4).

Acknowledgments

This work was supported by the National Institute of Health (J.M.S., E.D.S., F.R.C.), the Burroughs Wellcome Fund (J.S) and the National Science Foundation (E.D.S.). We thank N. Buchler, G. Charvin, B. Drapkin and J.E. Ferrell for insightful conversations, and J. Widom and C. Wittenberg for thoughtful comments on the manuscript. We thank J.M. Bean, B. Timney and J. Robbins for help with strain/plasmid construction, M. Schwab for the plasmid pWS358, B. Futcher for the *CLN2-NES* and *CLN2-NLS* plasmids, E. Bi for the pKT355 mCherry tagging plasmid, and M. Tyers for *WHI5* phosphorylation site mutant strains and plasmids. The authors declare no competing financial interests.

References

1. Simchen G, Pinon R, Salts Y. Sporulation in Saccharomyces cerevisiae: premeiotic DNA synthesis, readiness and commitment. Exp Cell Res 1972;75:207–18. [PubMed: 4564471]
2. Nachman I, Regev A, Ramanathan S. Dissecting timing variability in yeast meiosis. Cell 2007;131:544–56. [PubMed: 17981121]
3. Shenhar G, Kassir Y. A positive regulator of mitosis, Sok2, functions as a negative regulator of meiosis in Saccharomyces cerevisiae. Mol Cell Biol 2001;21:1603–12. [PubMed: 11238897]
4. Ferrell JE Jr, Machleder EM. The biochemical basis of an all-or-none cell fate switch in Xenopus oocytes. Science 1998;280:895–8. [PubMed: 9572732]
5. Xiong W, Ferrell JE Jr. A positive-feedback-based bistable 'memory module' that governs a cell fate decision. Nature 2003;426:460–5. [PubMed: 14647386]
6. Sha W, et al. Hysteresis drives cell-cycle transitions in Xenopus laevis egg extracts. Proc Natl Acad Sci U S A 2003;100:975–80. [PubMed: 12509509]

7. Pomerening JR, Sontag ED, Ferrell JE Jr. Building a cell cycle oscillator: hysteresis and bistability in the activation of Cdc2. Nat Cell Biol 2003;5:346–51. [PubMed: 12629549]
8. Hartwell LH, Culotti J, Pringle JR, Reid BJ. Genetic control of the cell division cycle in yeast. Science 1974;183:46–51. [PubMed: 4587263]
9. Johnston GC, Pringle JR, Hartwell LH. Coordination of growth with cell division in the yeast Saccharomyces cerevisiae. Exp Cell Res 1977;105:79–98. [PubMed: 320023]
10. Lord PG, Wheals AE. Variability in individual cell cycles of Saccharomyces cerevisiae. J Cell Sci 1981;50:361–76. [PubMed: 7033253]
11. Di Talia S, Skotheim JM, Bean JM, Siggia ED, Cross FR. The effects of molecular noise and size control on variability in the budding yeast cell cycle. Nature 2007;448:947–51. [PubMed: 17713537]
12. Jorgensen P, Tyers M. How cells coordinate growth and division. Curr Biol 2004;14:R1014–27. [PubMed: 15589139]
13. Tyers M, Tokiwa G, Futcher B. Comparison of the Saccharomyces cerevisiae G1 cyclins: Cln3 may be an upstream activator of Cln1, Cln2 and other cyclins. Embo J 1993;12:1955–68. [PubMed: 8387915]
14. Dirick L, Bohm T, Nasmyth K. Roles and regulation of Cln-Cdc28 kinases at the start of the cell cycle of Saccharomyces cerevisiae. Embo J 1995;14:4803–13. [PubMed: 7588610]
15. Stuart D, Wittenberg C. CLN3, not positive feedback, determines the timing of CLN2 transcription in cycling cells. Genes Dev 1995;9:2780–94. [PubMed: 7590253]
16. Spellman PT, et al. Comprehensive identification of cell cycle-regulated genes of the yeast Saccharomyces cerevisiae by microarray hybridization. Mol Biol Cell 1998;9:3273–97. [PubMed: 9843569]
17. Kato M, Hata N, Banerjee N, Futcher B, Zhang MQ. Identifying combinatorial regulation of transcription factors and binding motifs. Genome Biol 2004;5:R56. [PubMed: 15287978]
18. de Bruin RA, McDonald WH, Kalashnikova TI, Yates J 3rd, Wittenberg C. Cln3 activates G1-specific transcription via phosphorylation of the SBF bound repressor Whi5. Cell 2004;117:887–98. [PubMed: 15210110]
19. Costanzo M, et al. CDK activity antagonizes Whi5, an inhibitor of G1/S transcription in yeast. Cell 2004;117:899–913. [PubMed: 15210111]
20. Amon A, Tyers M, Futcher B, Nasmyth K. Mechanisms that help the yeast cell cycle clock tick: G2 cyclins transcriptionally activate G2 cyclins and repress G1 cyclins. Cell 1993;74:993–1007. [PubMed: 8402888]
21. de Bruin RA, et al. Constraining G1-specific transcription to late G1 phase: the MBF-associated corepressor Nrm1 acts via negative feedback. Mol Cell 2006;23:483–96. [PubMed: 16916637]
22. Cross FR, Tinkelenberg AH. A potential positive feedback loop controlling CLN1 and CLN2 gene expression at the start of the yeast cell cycle. Cell 1991;65:875–83. [PubMed: 2040016]
23. Dirick L, Nasmyth K. Positive feedback in the activation of G1 cyclins in yeast. Nature 1991;351:754–7. [PubMed: 1829507]
24. Bean JM, Siggia ED, Cross FR. Coherence and timing of cell cycle Start examined at single-cell resolution. Mol Cell 2006;21:3–14. [PubMed: 16387649]
25. Mateus C, Avery SV. Destabilized green fluorescent protein for monitoring dynamic changes in yeast gene expression with flow cytometry. Yeast 2000;16:1313–23. [PubMed: 11015728]
26. Samoilov MS, Price G, Arkin AP. From fluctuations to phenotypes: the physiology of noise. Sci STKE 2006 2006:re17.
27. Iyer VR, et al. Genomic binding sites of the yeast cell-cycle transcription factors SBF and MBF. Nature 2001;409:533–8. [PubMed: 11206552]
28. Harbison CT, et al. Transcriptional regulatory code of a eukaryotic genome. Nature 2004;431:99–104. [PubMed: 15343339]
29. Simon I, et al. Serial regulation of transcriptional regulators in the yeast cell cycle. Cell 2001;106:697–708. [PubMed: 11572776]
30. Koch C, Schleiffer A, Ammerer G, Nasmyth K. Switching transcription on and off during the yeast cell cycle: Cln/Cdc28 kinases activate bound transcription factor SBF (Swi4/Swi6) at start,

whereas Clb/Cdc28 kinases displace it from the promoter in G2. Genes Dev 1996;10:129–41. [PubMed: 8566747]

31. Moffat J, Andrews B. Late-G1 cyclin-CDK activity is essential for control of cell morphogenesis in budding yeast. Nat Cell Biol 2004;6:59–66. [PubMed: 14688790]
32. Zachariae W, Schwab M, Nasmyth K, Seufert W. Control of cyclin ubiquitination by CDK-regulated binding of Hct1 to the anaphase promoting complex. Science 1998;282:1721–4. [PubMed: 9831566]
33. Wijnen H, Landman A, Futcher B. The G(1) cyclin Cln3 promotes cell cycle entry via the transcription factor Swi6. Mol Cell Biol 2002;22:4402–18. [PubMed: 12024050]
34. Edgington NP, Futcher B. Relationship between the function and the location of G1 cyclins in S. cerevisiae. J Cell Sci 2001;114:4599–611. [PubMed: 11792824]
35. Miller ME, Cross FR. Distinct subcellular localization patterns contribute to functional specificity of the Cln2 and Cln3 cyclins of Saccharomyces cerevisiae. Mol Cell Biol 2000;20:542–55. [PubMed: 10611233]
36. Koch C, Moll T, Neuberg M, Ahorn H, Nasmyth K. A role for the transcription factors Mbp1 and Swi4 in progression from G1 to S phase. Science 1993;261:1551–7. [PubMed: 8372350]
37. Bean JM, Siggia ED, Cross FR. High Functional Overlap Between MBF and SBF in the G1/S Transcriptional Program in Saccharomyces cerevisiae. Genetics. 2005
38. McCusker D, et al. Cdk1 coordinates cell-surface growth with the cell cycle. Nat Cell Biol 2007;9:506–15. [PubMed: 17417630]
39. Polymenis M, Schmidt EV. Coupling of cell division to cell growth by translational control of the G1 cyclin CLN3 in yeast. Genes Dev 1997;11:2522–31. [PubMed: 9334317]
40. Wang H, Gari E, Verges E, Gallego C, Aldea M. Recruitment of Cdc28 by Whi3 restricts nuclear accumulation of the G1 cyclin-Cdk complex to late G1. Embo J 2004;23:180–90. [PubMed: 14685274]
41. Schneider BL, Yang QH, Futcher AB. Linkage of replication to start by the Cdk inhibitor Sic1. Science 1996;272:560–2. [PubMed: 8614808]
42. Lanker S, Valdivieso MH, Wittenberg C. Rapid degradation of the G1 cyclin Cln2 induced by CDK-dependent phosphorylation. Science 1996;271:1597–601. [PubMed: 8599119]
43. Shaner NC, et al. Improved monomeric red, orange and yellow fluorescent proteins derived from Discosoma sp. red fluorescent protein. Nat Biotechnol 2004;22:1567–72. [PubMed: 15558047]

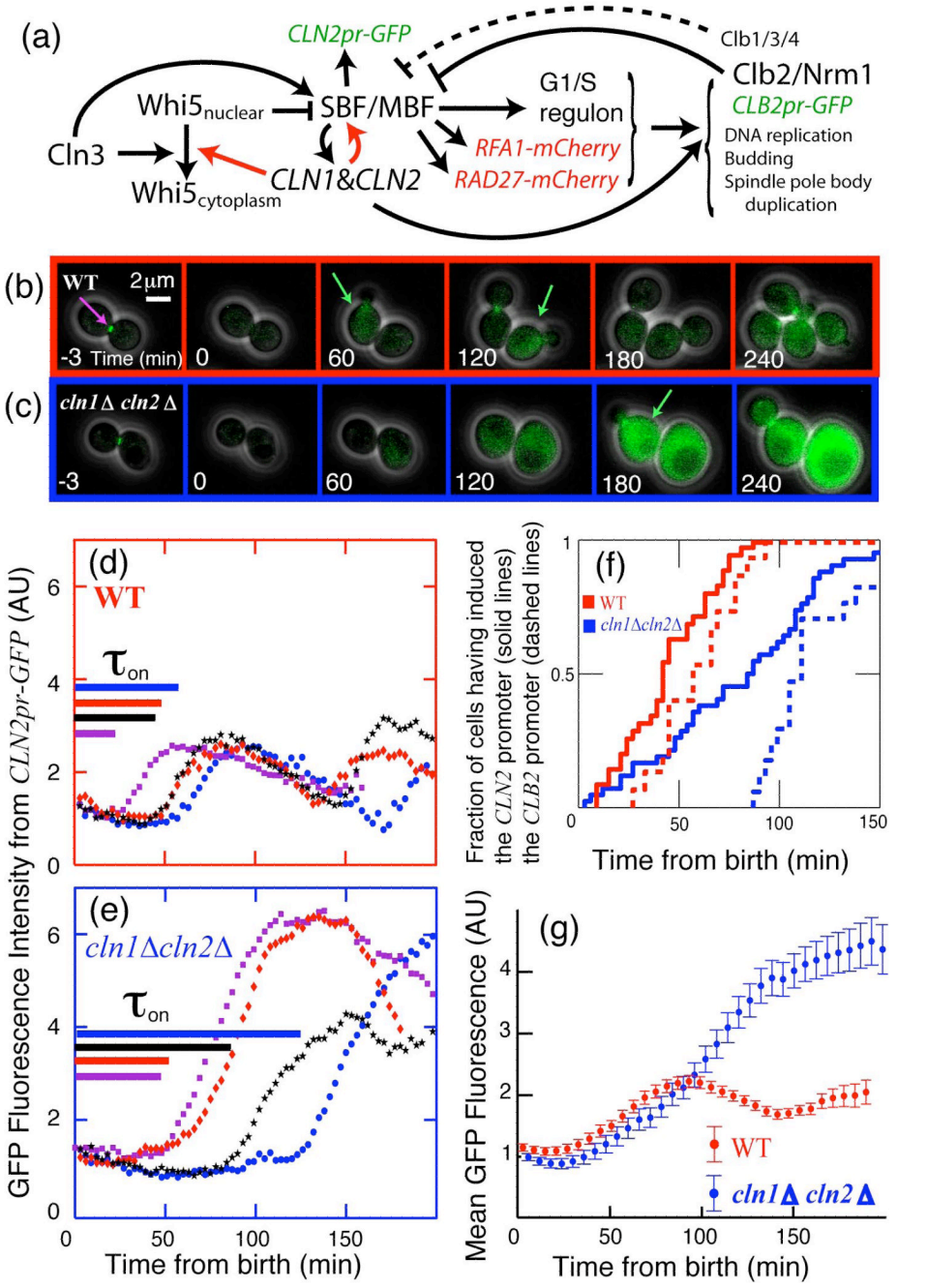

Figure 1. Positive feedback drives the Start of the budding yeast cell cycle

(a) Schematic of the Start transition; novel interactions demonstrated in this paper are shown in red. (b,c): Combined phase and fluorescent images for *CLN2pr-GFP MYO1-GFP MET3pr-CLN2* cells, either wild type (b) or *cln1*Δ *cln2*Δ (c), grown in -Met (inducing) and plated on +Met (repressing) to normalize initial conditions[6] (Fig. S3). Green arrows indicate approximate peak GFP expression from *CLN2pr-GFP*. (d,e): Single-cell fluorescence intensity for 4 characteristic cells of each genotype; cells are synchronized at birth, marked by the disappearance of a Myo1-GFP ring at the bud-neck (purple arrow in a). Time from birth to *CLN2* promoter activation (as defined in Methods),$\tau_{on,}$ for each individual cell is indicated by length of the corresponding line in (d,e). (f) Cumulative distribution of

CLN2pr-GFP induction (solid lines) indicates that Cln1,2-dependent positive feedback contributes substantially to the early expression of *CLN2*; dashed lines indicate induction of *CLB2pr-GFP* marking the onset of negative regulation of *CLN2*. (g) Averaging fluorescence intensity for 87 WT and 83 *cln1*Δ *cln2*Δ daughter cells aligned at birth simulates a population study, which would obscure the effect of positive feedback. The results shown are for daughter cells in glucose; changes in cell type or nutrient conditions do not qualitatively influence the results (Table S3).

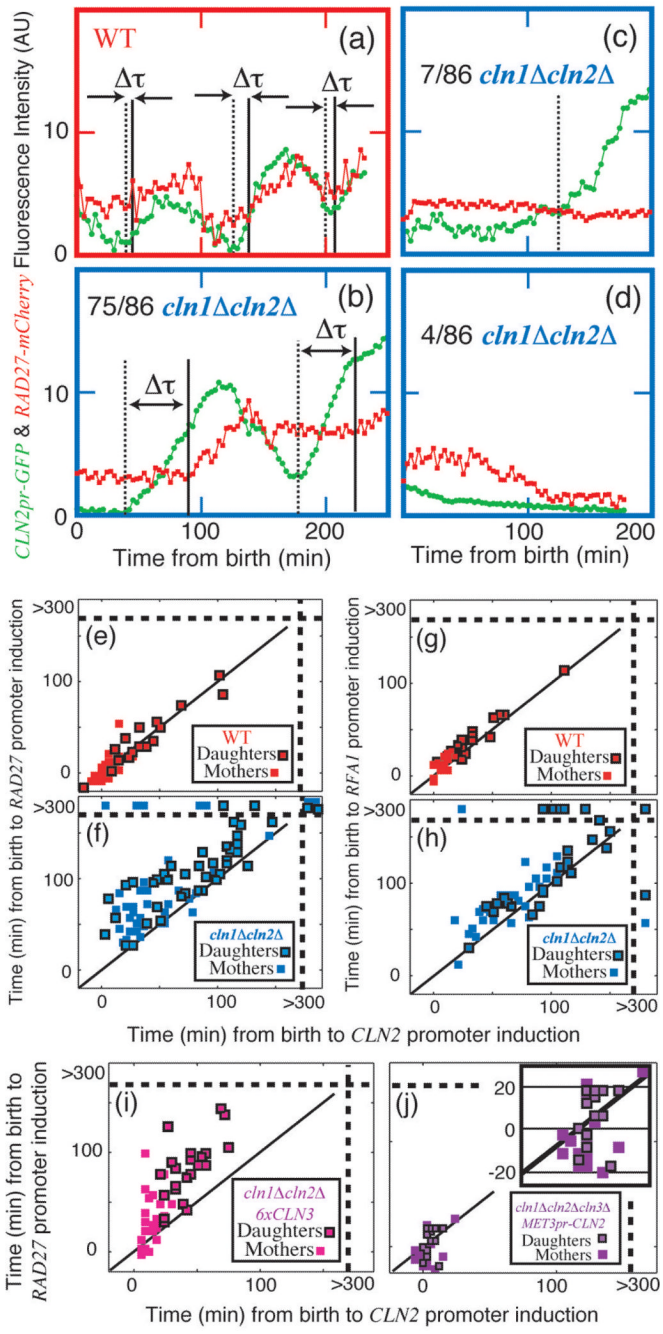

Figure 2. Cln1,2 drive coherent expression of the SBF/MBF regulon

(a–f): Strains containing both *CLN2pr-GFP* (green) and *RAD27-mCherry* (red) were examined (see Supplementary Information for detailed methods); τ marks the computed time between *CLN2* and *RAD27* inductions. WT (a, e): all cells transcribed both markers synchronously. *cln1*Δ *cln2*Δ, (b–d, f): 75 cells transcribed both markers, with variable intervening intervals; 7 cells transcribed *CLN2pr-GFP*, but not *RAD27-mCherry*; and 4 cells transcribed neither. Correlation of the initiation of *RAD27* and *CLN2* transcription in WT (e) and *cln1*Δ *cln2*Δ (f); points beyond the dotted lines in (f) represent no transcription within 300 min (movie limit; see also Table S3). (g–h): Substituting *RFA1-mCherry* for *RAD27-mCherry* yielded similar results. (i) *cln1*Δ *cln2*Δ *6xCLN3* cells and (j) *cln1*Δ *cln2*Δ *cln3*Δ

cells expressing *CLN2* from a *MET3* promoter exhibited incoherent regulon expression compared to WT, although expression of both *CLN2pr* and *RAD27pr* were faster than in *cln1*Δ *cln2*Δ. $P < 10^{-3}$ for all comparisons.

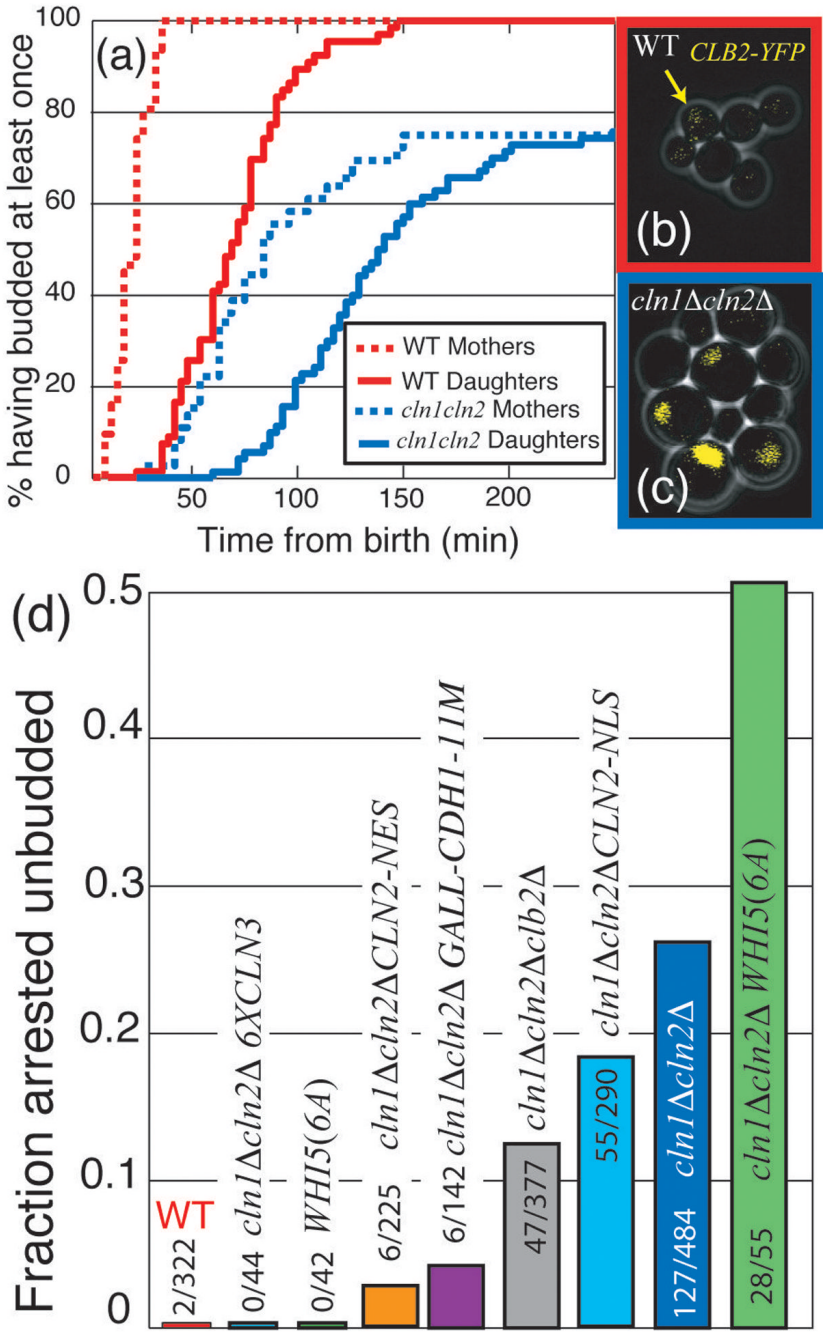

Figure 3. Stochastic unbudded arrest in *cln1*Δ *cln2*Δ cells, and its modulation by mitotic cyclins, Whi5, Cln3, and Cln2

(a) Cumulative plot of percentage of cells that budded at least once: 26% of *cln1*Δ *cln2*Δ cells arrest unbudded. (b,c): cells with integrated *CLB2-YFP* fusion protein (endogenous promoter); WT (b) and *cln1*Δ *cln2*Δ (c). Note high nuclear Clb2 specifically in large unbudded (arrested) *cln1*Δ *cln2*Δ cells. (d) Delaying (*cln1*Δ *cln2*Δ *clb2*Δ) or removing (*cln1*Δ *cln2*Δ *GALL-CDH1-11M*) mitotic cyclin accumulation reduced the fraction of arrested cells; addition of 5 copies of *CLN3* eliminated this arrest, while the addition of *WHI5(6A)* exacerbated the arrest. Unbudded arrest was weakly rescued by nuclear Cln2

(*CLN2-NLS*), and strongly rescued by cytoplasmic Cln2 (*CLN2-NES*). Unless stated otherwise in text $P < 10^{-3}$ for all comparisons.

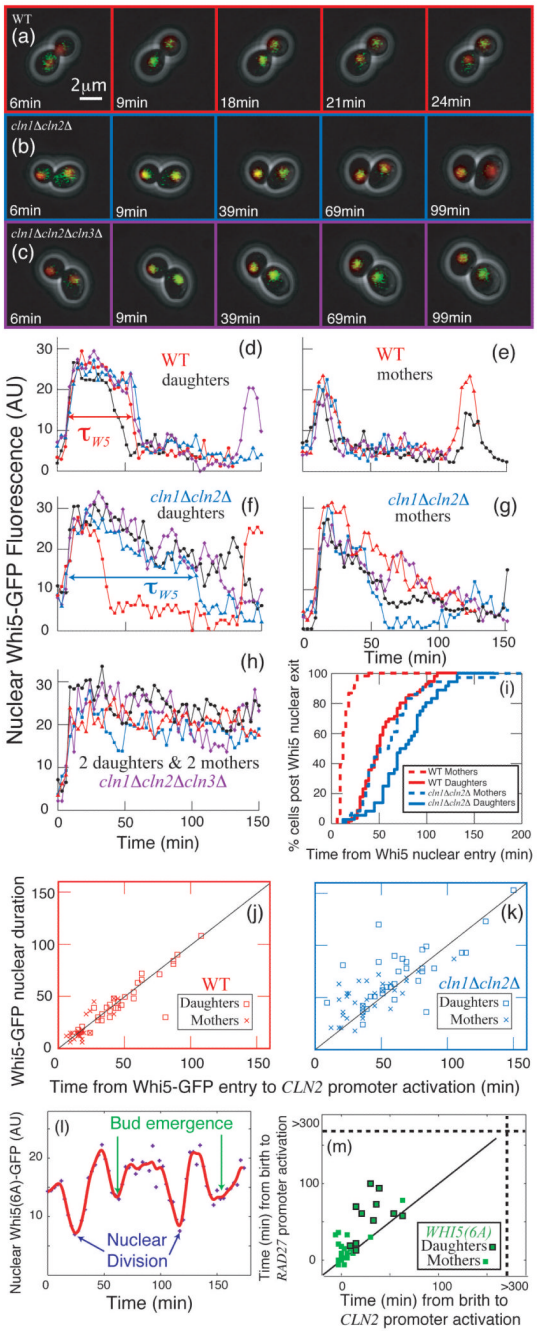

Figure 4. Cln1,2 are required for rapid phosphorylation and inactivation of the rate- limiting repressor Whi5

(a–c): Combined phase and fluorescent images showing Whi5- GFP and Htb2-mCherry (to mark the nucleus) fusion proteins for (a) WT, (b) *cln1*Δ *cln2*Δ, and (c) *cln1*Δ *cln2*Δ *cln3*Δ cells. The difference between nuclear and non-nuclear fluorescence intensity was used to quantify nuclear Whi5 by automated image analysis. Compared to WT (d,e), in *cln1*Δ ^{cln2}Δ cells (f,g), Whi5 nuclear exit occurs later and is less sharp. In *cln1*Δ *cln2*Δ *cln3*Δ cells, Whi5 remains nuclear (h). (i) Percent of cells in which Whi5 has left the nucleus (defined as attaining half the maximum level) versus the time from Whi5 nuclear entry. (j,k) Whi5 nuclear exit is tightly correlated with *CLN2* promoter activation in WT cells and less

correlated in *cln1*Δ *cln2*Δ cells (See also Table S3). (l) *WHI5(6A)-GFP*[19], lacking 6 out of 12 Cln-dependent phosphorylation sites, reproducibly displayed significant, but slower and incomplete, shuttling out of the nucleus at Start and again at nuclear division. In *WHI5(6A)* strains containing *CLN2pr-GFP* and *RAD27-mCherry* (m), *CLN2* and *RAD27* induction were incoherent, correlating with the poor nuclear transport of Whi5(6A)-GFP.

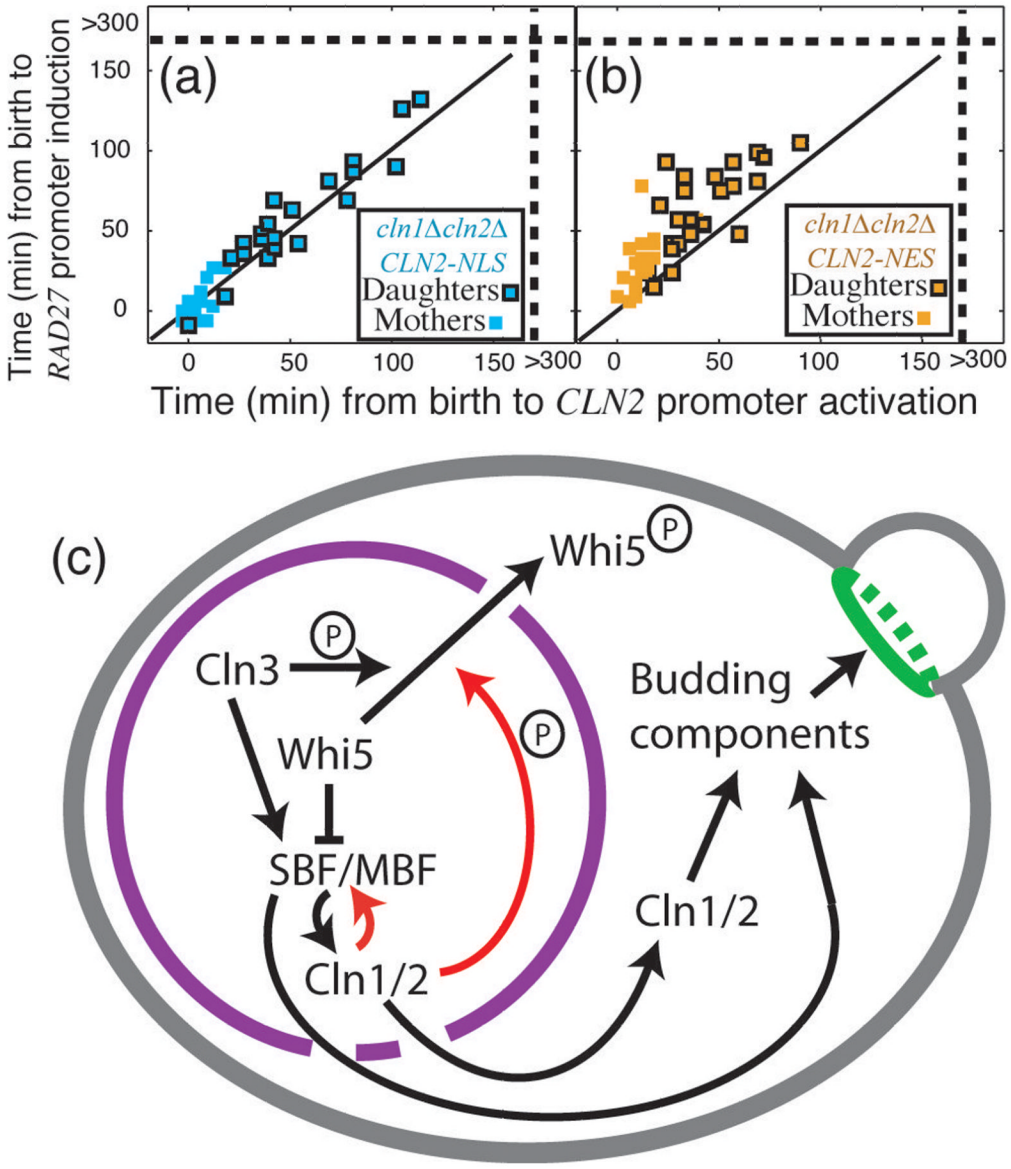

Figure 5. Function of nuclear Cln2 and model for Start regulation by positive feedback

Comparison of *cln1*Δ *cln2*Δ cells with either a nuclear localized (a) or a nuclear excluded (b) *CLN2* allele suggests that nuclear Cln2 is necessary and sufficient for regulon coherence. Strains contained *CLN2pr-GFP* and *RAD27-mCherry*. (c) Model for regulon activation and bud emergence: red lines indicate